Research Article

Application of blocked-off method to simulate laminar forced convection flow in a channel with variable cross-section

A R Hodjat[1], M Atashafrooz[2*]

[1]Department of Mechanical Engineering, Bardsir Branch, Islamic Azad University, Kerman, IRAN
[2]Department of Mechanical Engineering, Shahid Bahonar University, Kerman, IRAN.
Email: hojat@bardsiriau.ac.ir, meysam.atashafrooz@gmail.com

Abstract

This paper presents a numerical investigation of laminar forced convection flow in a duct with variable cross-section. These various cross-sections are simulated with a recess including two inclined backward and forward facing steps (BFS and FFS). To simulate the inclined surfaces of the FFS and BFS, the blocked off method is employed. To solve the governing equations including the conservations of mass, momentum and energy, the two-dimensional Cartesian coordinate system is used. Discretized forms of these equations are obtained by the finite volume method and solved using the SIMPLE algorithm. The numerical results are presented graphically and the effects of step inclination angle, recess length and Reynolds number as the main parameters on the flow and heat transfer behaviors of the system are investigated. Comparison of numerical results with the available data published in open literature shows good consistency.

Keywords: Backward and forward facing inclined steps, Laminar forced convection, Recess, Blocked off method.

[*]**Address for Correspondence:**
Dr. M. Atashafrooz, Department of Mechanical Engineering, Bardsir Branch, Islamic Azad University, Kerman, IRAN.
Email: meysam.atashafrooz@gmail.com
Received Date: 11/10/2014 Accepted Date: 21/10/2014

Access this article online

Quick Response Code:

Website: www.statperson.com

DOI: 30 October 2014

INTRODUCTION

Forced convection flow in a duct with variable cross-section is widely encountered in engineering applications. In many cases, the various cross-sections in duct flows are created by backward or forward facing steps. Separation flows accompanied with heat transfer are frequently encountered in several engineering application, such as heat exchangers, gas turbine blades, combustion chamber and ducts flows used in industrial applications. A great deal of fluid mixing in the separated region has a considerable effect on the flow and heat transfer performances of these devices. Therefore, the studies on separated flows both theoretically and experimentally have been conducted extensively during the past decade. The flow over backward-facing step (BFS) or forward-facing step (FFS) has the most features of separated flows. There are many studies in which the BFS or FFS flows were analyzed from a fluid mechanics or a heat transfer perspective. Although the geometry of BFS or FFS flow is very simple, the heat transfer and fluid flow over this type of step contain most of complexities. Consequently, it has been used in the benchmark investigations. There are many studies about laminar convection flow over BFS in a duct by several investigators[1-4]. Kondoh *et al*.[5] studied laminar heat transfer in a separating and reattaching flow, numerically, by simulating the flow and heat transfer downstream of a backward-facing step. The effects of channel expansion ratio, Reynolds number and Prandtl number on heat transfer behavior were investigated. Erturk[6] investigated the characteristics of the flow over a two dimensional BFS in a wide range of Reynolds numbers. The two-dimensional Navier–Stokes equations for incompressible steady flows were solved with a very efficient finite

How to site this article: A R Hodjat, M Atashafrooz. Application of blocked-off method to simulate laminar forced convection flow in a channel with variable cross-section. *International Journal of Statistika and Mathemtika* Nov 2014 to Jan 2015; 12(1): 41-49. http://www.statperson.com (accessed 01 November 2014).

difference numerical method which proved to be highly stable even at very high Reynolds numbers. Abu-nada[7-9] analyzed the convection flow over a backward facing step in a duct to investigate the amount of entropy generation in this type of flow. In those works, the set of governing equations were solved by the finite volume method and the distributions of entropy generation number, friction coefficient and Nusselt number on the duct walls were calculated. Moreover, the effect of suction and blowing on the entropy generation number and Bejan number were presented. Although there are many research studies about BFS geometries, the fluid flow with heat transfer over forward facing step (FFS) received less attention in comparison to the convection flow over backward facing step. In FFS flow, depending on the magnitude of the Reynolds number and geometrical factors, one or two separated flow regions may develop adjacent to the step surface. These separated flow regions make this geometry more complicated to study than the BFS flow in which only one separated flow region occurs behind the step. Owing to this fact, very limited number of research works has investigated the laminar convection flow over FFS in contrast to the BFS geometry. In a recent study, Bahrami and Gandjalikhan Nassab[10] analyzed the convection flow over forward facing step in a duct to investigate the amount of entropy generation in this type of flow. A review of research on laminar convection flow over backward and forward facing steps was done by Abu-Mulaweh[11]. In that study, a comprehensive review of such flows, those have been reported in several studies in the open literature was presented. The purpose was to give a detailed summery of the effect of several parameters such as step height, Reynolds number, Prandtl number and the buoyancy force on the flow and temperature distributions downstream of the step. Also at different points of view, this geometry (FFS) was studied by several researchers[12-13]. In all of the above works, the step was considered to be vertical to the bottom wall. There are many engineering applications in which the forward or backward facing step is inclined. Simulations of three-dimensional laminar forced convection adjacent to inclined backward-facing step in rectangular duct were presented by chen *et al.*[14] to examine the effects of step inclination on flow and heat transfer distributions. Velocity, temperature, Nusselt number and friction coefficient distributions were presented in that study. The effects of step inclination angle on Nusselt number and friction coefficient distributions were showed by plotting many figures. In a recent study, Gandjalikhan Nassab *et al.*[15] studied the turbulent forced convection flow adjacent to inclined forward facing step in a duct. In that study, the Navier-Stokes and energy equations were solved in the computational domain by CFD method using conformal mapping technique and the effects of step inclination angle on flow and temperature distributions were determined. Ansari and Gandjalikhan Nassab[16] studied the laminar forced convection flow of a radiating gas adjacent to inclined forward facing step in a duct. In that study the blocked-off method was used to simulate the inclined step. The effect of radiative parameters on thermal behavior of fluid flow was studied. As the convection flow in a duct with variable cross-section has many applications in engineering, the present work deals the analysis of laminar forced convection flow in this geometry. Although this geometry has many applications in thermal system such as cooling of electronic devices, in which the gas flow experiences both expansion and contraction in a duct, but this type of convection flow has not been studied by any investigator.

PROBLEM DESCRIPTION

The geometric model used in this study (Figure 1) is a duct with variable cross-section. These cross-sections are simulated by a recess including two inclined BFS and FFS. According to Fig. 1 the upstream and downstream heights of the duct are h_1 and h_2 respectively. The height of the duct inside the recess region is H such that this geometry provides the step height of s, with expansion ($ER=H/h_1$) and contraction ($CR=h_2/H$) ratios of 2 and 0.5, respectively. The upstream length of the duct is considered to be $L_1=10H$ and the rest of the channel length is equal to $L_2=30H$. This is made to ensure that the flow at the inlet and outlet section is not affected significantly by the sudden changes in the geometry and flow at the exit section becomes fully developed. The length of recess depicted by D is considered to be 5H and 20H in the computations. Also the step inclination angle indicated by Φ is considered to be 30, 45, 60 and 90° in subsequent test cases.

BASIC EQUATIONS

For incompressible, steady and two-dimensional laminar flow, the governing equations are the conservations of mass, momentum and energy that can be written as follows:

$$\frac{\partial u}{\partial x}+\frac{\partial v}{\partial y}=0 \tag{1}$$

$$u\frac{\partial u}{\partial x}+v\frac{\partial u}{\partial y}=-\frac{1}{\rho}\frac{\partial p}{\partial x}+\frac{\mu}{\rho}\left(\frac{\partial^2 u}{\partial x^2}+\frac{\partial^2 u}{\partial y^2}\right) \tag{2}$$

$$u\frac{\partial v}{\partial x}+v\frac{\partial v}{\partial y}=-\frac{1}{\rho}\frac{\partial p}{\partial y}+\frac{\mu}{\rho}\left(\frac{\partial^2 v}{\partial x^2}+\frac{\partial^2 v}{\partial y^2}\right) \quad (3)$$

$$u\frac{\partial T}{\partial x}+v\frac{\partial T}{\partial y}=\alpha\left(\frac{\partial^2 T}{\partial x^2}+\frac{\partial^2 T}{\partial y^2}\right) \quad (4)$$

In the above equations, u and v are the velocity components in x- and y- directions, p the pressure and T is the temperature respectively. In addition, ρ is the density, μ the dynamic viscosity and α is the thermal diffusivity of fluid which are all kept constant in this study.

Boundary Condition

The boundary conditions are treated as no slip conditions at the solid walls (zero velocity) and constant temperature of T_w at the bottom and top walls including the step surfaces. At the inlet duct section, the flow is fully developed with uniform temperature of T_{in}, which is assumed to be lower than T_w. At the outlet section, zero axial gradients for velocity components and gas temperature are employed.

Non-Dimensional Forms the Governing Equations

In numerical solution of the set of governing equations including the continuity, momentum and energy, the following dimensionless parameters are used to obtain the non-dimensional forms of these equations:

$$(X,Y)=\left(\frac{x}{D_h},\frac{y}{D_h}\right),(U,V)=\left(\frac{u}{U_\circ},\frac{v}{U_\circ}\right),P=\frac{p}{\rho U_\circ^2},$$
$$\Theta=\frac{T-T_{in}}{T_w-T_{in}},Pr=\frac{\nu}{\alpha},Re=\frac{\rho U_\circ D_h}{\mu},Pe=Re.Pr \quad (5)$$

Where D_h is the hydraulic diameter which is equal to $2h_1$. The non-dimensional forms of the governing equations are as follows:

$$\frac{\partial U}{\partial X}+\frac{\partial V}{\partial Y}=0 \quad (6)$$

$$\frac{\partial}{\partial X}\left(U^2-\frac{1}{Re}\frac{\partial U}{\partial X}\right)+\frac{\partial}{\partial Y}\left(UV-\frac{1}{Re}\frac{\partial U}{\partial Y}\right)=-\frac{\partial P}{\partial X} \quad (7)$$

$$\frac{\partial}{\partial X}\left(UV-\frac{1}{Re}\frac{\partial V}{\partial X}\right)+\frac{\partial}{\partial Y}\left(V^2-\frac{1}{Re}\frac{\partial V}{\partial Y}\right)=-\frac{\partial P}{\partial Y} \quad (8)$$

$$\frac{\partial}{\partial X}\left(U\Theta-\frac{1}{Pe}\frac{\partial \Theta}{\partial X}\right)+\frac{\partial}{\partial Y}\left(V\Theta-\frac{1}{Pe}\frac{\partial \Theta}{\partial Y}\right)=0 \quad (9)$$

In the present study, physical quantities of interest in flow field and heat transfer study are the friction coefficient and Nusselt number. These parameters along with the modified friction coefficient can be expressed as:

$$Nu=-\frac{1}{(\Theta_b-\Theta_w)}\left.\frac{\partial \Theta}{\partial Y}\right|_{Y=0.0} \quad \text{where} \quad \Theta_b=\frac{\int_0^1 U\Theta dY}{\int_0^1 U dY} \quad (10)$$

$$C_f=\frac{2}{Re}\left.\frac{dU}{dY}\right|_{Y=0.0} \quad (11)$$

$$C_f^*=\frac{Re}{2}C_f \quad (12)$$

NUMERICAL PROCEDURE

Discretized forms of the partial differential equations[6] to[9] were obtained by integrating over an elemental cell volume with staggered control volumes for the x- and y-velocity components. Other variables of interest were computed at the grid nodes. The discretized forms of the governing equations were numerically solved by the SIMPLE algorithm of Patankar and Spalding[17] using the Hybrid method (please see appendix). Numerical calculations were performed by writing a computer program in FORTRAN Based on the result of grid tests for obtaining the grid-independent solutions, six different

meshes were used in the grid independence study. The corresponding maximum value of the total Nusselt number on the bottom wall and also the location of reattachment point are calculated and tabulated in Table I. As it is seen, a grid size of 800×40 can be chosen for obtaining the grid independent solution, such that the subsequent numerical calculations are made based on this grid size. It should be mentioned that near the top, bottom and step walls clustering is employed in the x- and y-directions for obtaining more accuracy in the numerical calculations. To simulate the inclined surfaces in the computational domain, the blocked off method is used in this study (see Fig. 2). Numerical solutions are obtained iteratively by the line-by-line method such that iterations are terminated when sum of the absolute residuals is less than 10^{-4} for each equation. By this numerical strategy, the velocity and temperature distributions in the fluid flow can be obtained.

BLOCKED OFF METHOD

In many cases, a computer program written for a regular grid can be improved to handle an irregularly shaped computational domain using the blocked-off method[18]. In this technique, the whole 2-D region is divided into two parts: active and inactive or blocked-off regions. The region where solutions are done is known as the active region and the remaining portion is known as the inactive or the blocked-off region. Therefore, by rendering inactive some of the control volumes of the regular grid, the remaining active control volumes form the desired irregular domain with complex boundary. By this technique, the surfaces of inclined steps in the present analysis are approximated by a series of fine rectangular steps, Fig. 2. It should be mentioned that the control volumes, which are inside the active region, are designated as 1 and otherwise they are 0, as shown in Fig. 2. It is obvious that using fine grids in the interface region between active and inactive zones causes to have an approximated boundary which is more similar to the true boundary.

According to the blocked-off technique, known values of the dependent variables must be established in all inactive control volumes. If the inactive region represents a stationary solid boundary as in the case, the velocity components in that region must be equal to zero, and if the region is regarded as isothermal boundary, the known temperature must be established in the inactive control volumes.

VALIDATION OF COMPUTATIONAL RESULTS

The present numerical implementation was validated by reproducing the results of two authors in which a forced convection flow of gas over a BFS was studied. The results of reattachment point in flow over BFS with an expansion ratio of 2 and for different Reynolds numbers are compared with the experimental data, obtained by Armaly *et al.*[1], in Fig. 3(a). As this figure shows, the reattachment point moves toward the downstream side as the Reynolds number increases. However, a good consistency is seen between experimental and present numerical results. To compare the results of heat transfer, another test case is studied in BFS, in which the bottom wall was permeable with bleeding condition, including both suction and blowing. Variation of Nusselt number along the bottom wall is compared with that obtained by Abu-Nada[9], in the case of ER=2, Re = 400 and no permeable condition. The results are presented graphically in Fig. 3(b). In this test case, the temperature of the top wall was lower than the temperature of the bottom wall and the gas temperature profile at the inlet section was assumed to be fully developed. The variation of Nusselt number shows that the convection coefficient increases after the step up to the reattachment point in which the maximum value of Nusselt number takes place and then Nu decreases and approaches to a fixed value far from the step. However, Fig. 3(b) shows a good consistency between the present numerical results with those reported by Abu-Nada[9].

RESULT AND DISCUSSION

The present research results are about an air flow in a duct with two subsequent expansion ratio of ER=2 and contraction ratio of CR=0.5 with two lengths for the recess region and various angles for the inclined steps (30, 45, 60 and 90°). In addition, the Reynolds number is varied between 100 and 600, while the Prandtl number is kept constant at 0.71 to guarantee constant fluid physical properties for moderate and small values of temperature difference. First in order to show the flow pattern, the streamlines are plotted in Fig. 4 while the recess length is equal to D=20H. The effect of sudden expansion and contraction along two steps is clearly seen from the curvatures of streamlines. Fig. 4(a) shows that three main recirculation zones are encountered for the step inclination angle of $\phi = 90^\circ$ for Re=400 in the flow domain. The primary recirculation region occurs downstream the backward step adjacent the bottom wall, whereas the secondary recirculation zone exists along the top wall and the third recirculation region occurs on the bottom wall before the forward step and adjacent to the step corner. It should be noted that for small values of Reynolds number (say for Re<350 for this test case), the secondary recirculation zone disappears. To see the effect of step inclination angle on the fluid flow behavior, Fig. 4(b) shows the streamline contours for $\phi = 30^\circ$. It can be seen from this figure that by decreasing step inclination angle, the length of reattachment point decreases and

third recirculation region disappears while the effect of secondary bubble region decreases. The variations of Nusselt number along the bottom wall at Re = 400 and in different step inclination angles are illustrated in Fig. 5. This figure shows that after the backward step location, the value of Nu increases sharply in the primary recirculated region because of the flow vortices, such that the maximum local Nusselt number on the bottom wall coincides with the point of reattachment after which Nusselt number decreases and approaches to a constant value as the distance continues to increase in the stream-wise direction. Then, the Nusselt number decreases along the flow direction such that the value of Nusselt number vanishes at the forward step corner where the fluid has no any motion. Moreover, Fig. 5 shows the effect of step inclination angle on the distribution of Nusselt number along the bottom wall. This figure shows that the increase of step inclination angle, increases the maximum local Nusselt number which is due to the increased vortices rate in primary recirculation region. High values of vortices results in higher convection coefficient, as is shown in Fig. 5. Fig. 6 presents the distribution of modified friction coefficient [9] on the bottom wall for various values of the step inclination angle at Re = 400. It is obvious that the coefficient of friction is negative inside the recirculation domain due to the back flow. The back flow is recognized by the negative values of velocity and negative velocity gradients. At the point of reattachment, the coefficient of friction is zero due to the vanished velocity gradients. In addition, at the step corners where the flow is at rest, the coefficient of friction becomes zero. By examining the effect of step inclination angle on friction coefficient within the recirculation region, it is clear that by decreasing the step inclination angle, the maximum coefficient of friction decreases. This is due to the repulsion of streamlines from the bottom wall. Before the reattachment point, increase of step inclination angle, increases the coefficient of friction due to increase of velocity gradient.To study the effect of recess length on the flow and heat transfer behaviors of convection flow, another test case with the same Reynolds number (Re=400) is also analyzed for a short recess length with D=5H. To have a better view of the flow pattern, the streamlines contours for D=5H and for the various step inclination angles are plotted in Fig. 7. If one compares the streamlines in Fig. 7 with those plotted in Fig. 4, it can be concluded that the flow field has different patterns in long and short recess lengths, such that it is seen that the recess length has a great effect on the flow pattern. In this test case, because of short recess length D, the secondary recirculation region disappears while primary and third recirculation regions affect each other, such that when the step inclination angle increases, the negative velocity and negative velocity gradient exist throughout the bottom wall which causes negative value of friction coefficient along this surface, as is shown in Fig. 8. Figure 9 shows the distribution of Nusselt number along the bottom wall. Comparison of this figure with Nu distribution shown in Fig. 5 illustrates that Nu distribution has different trends in short and long recess. As it is seen from this figure, the Nusselt number increases after the backward step in the primary recirculation region and reaches to its maximum value nearly at the end of primary recirculation region and then decreases to its minimum value at the forward step corner where the flow is at rest. It is important to note that by increasing step inclination angle high convection coefficients produced along the heated wall. To study the effect of Reynolds number on the flow and heat transfer behaviors of fluid flow, distributions of streamlines, modified friction coefficient and Nusselt number are depicted in D=20H at constant step inclination angle in Figs. 10-12. Figure 10 shows the effect of Reynolds number on the streamlines contours which are plotted at three different Reynolds numbers of Re=200, 400 and 600. This figure shows that the value of reattachment length increases as the Reynolds number increases and also for high Reynolds numbers, the secondary recirculation region appears along the top wall. The variation of Nusselt number along the recess bottom wall is plotted in Fig. 11 at different Reynolds numbers. As it is seen from this figure, by increasing the Reynolds number, the maximum Nusselt number increases and its location moves toward the downstream. Figure 12 shows the effect of Reynolds number on the friction coefficient on the recess bottom wall. This figure shows that the friction coefficient increases in primary recirculation region when Reynolds number increases, which is due to increased in the flow vortices inside this region. It is important to note that for the case of high Reynolds numbers, the coefficient of friction reaches a peak after the reattachment point. This peak coincides with the appearance of the secondary recirculation region on the top wall. The top secondary region narrows down the flow passage and maximizes local velocity gradients on the bottom wall.

CONCLUSION

The present research study deals the analysis of laminar forced convection flow in a duct with variable cross-section. These various cross-sections are simulated with a recess including two inclined BFS and FFS. The set of governing equations consisting of mass, momentum and energy is solved numerically by the techniques presented in computational fluid dynamic in the Cartesian coordinate system. The blocked off method is used in to simulate the inclined surfaces of FFS and BFS. The

effects of step inclination angle, recess length and Reynolds number on the Nusselt number and friction coefficient distribution along the bottom wall between the steps were investigated. It was revealed that these parameters have great effects on the flow field and thermal behavior of the duct flow. It was revealed that in long recess lengths, the maximum Nusselt number and friction coefficient increase by increasing in step inclination angle. But in the short recess lengths, as the primary and third recirculation region affect each other such that different behavior was seen.

REFERENCES

1. B. F. Armaly, F. Durst, JCF. Pereira and B. chonung, Experimental and theoretical investigation of backward-facing step flow, Journal of Fluid Mechanics, vol. 127 , pp. 473-496, 1983.
2. G. Vradis, and V. L. Nostrand, Laminar coupled flow downstream an asymmetric sudden expansion, Journal of Thermophysics Heat Transfer, vol. 6(2), pp. 288-295, 1992.
3. N. Tylli, L. Kaiktsis, B. Ineichen, Side wall effects in flow over backward-facing step: experiments and numerical solutions, Physics Fluids, vol. 14(11), pp. 3835-3845, 2002.
4. D. Brakely, M. Gabriela, M. Gomes and R. D. Henderson, Three - dimensional instability in flow over a backward - facing step, Journal of Fluid Mechanics, vol. 473, pp. 167-190, 2002.
5. T. Kondoh, Y. Nagano and T. Tsuji, Computational study of laminar heat transfer downstream of a backward-facing step, International Journal of Heat and Mass Transfer, vol. 36(3), pp. 577-591, 1993.
6. E. Erturk, Numerical solutions of 2-D steady incompressible flow over a backward-facing step, Part I: High Reynolds number solutions, Computers and Fluids, vol. 37, pp. 633–655, 2008.
7. E. Abu-Nada, "Numerical prediction of entropy generation in separated flows," Entropy, vol. 7, pp. 234–52, 2005.
8. E. Abu-Nada, "Entropy generation due to heat and fluid flow in backward facing step flow with various expansion ratios," International Journal of Exergy, vol. 3, pp. 419–35, 2006.
9. E. Abu-Nada, Investigation of entropy generation over a backward facing step under bleeding conditions, Energy Conversion and Management, vol. 49, pp. 3237–3242, 2008.
10. A. Bahrami, and S. A. Gandjalikhan Nassab, Study of Entropy Generation in Laminar Forced Convection Flow over a Forward-Facing Step in a Duct, International Review of Mechanical Engineering, vol. 4(4), pp. 399-404, 2010.
11. H. I. Abu- Mulaweh, A review of research on laminar mixed convection flow over backward- and forward-facing steps, International Journal of Thermal Sciences, vol. 42, pp. 897-909, 2003.
12. H.I. Abu-Mulaweh, Turbulent mixed convection flow over a forward-facing step-the effect of step heights, International Journal of Thermal Sciences, vol. 44, pp. 155–162, 2005.
13. I. Yilmaz, and H.F. Öztop, Turbulence forced convection heat transfer over double forward facing step flow, International Communications in Heat and Mass Transfer, vol. 33, pp. 508-517, 2006.
14. Y.T. Chen, J.H. Nie, H.T. Hsieh, and L.J. Sun, Three-dimensional convection flow adjacent to inclined backward-facing step, International Journal of Heat and Mass Transfer, vol. 49, pp. 4795–4803, 2006.
15. S. A. Gandjalikhan Nassab, R. Moosavi, and S. M. Hosseini Sarvari, Turbulent forced convection flow adjacent to inclined forward step in a duct, International Journal of Thermal Sciences, vol. 48, pp. 1319–1326, 2009.
16. A. B. Ansari, and S. A. Gandjalikhan Nassab, Numerical analysis of laminar forced convection flow of a radiating gas over an inclined forward facing step, International Review of Mechanical Engineering, vol. 5(1), pp. 120-127, 2011.
17. S. V. Patankar, and D. B. Spalding, A calculation procedure for heat, mass and momentum transfer in three-dimensional parabolic flows, International Journal of Heat and Mass Transfer, vol. 15(10), pp. 1787–1806, 1972.
18. S. V. Patankar, Numerical Heat Transfer and Fluid Flow, Taylor and Francis, Philadelphia, PA, Chap.7, 1981.

Source of Support: None Declared
Conflict of Interest: None Declared

APPENDIX

The hybrid method was developed by Patankar and Spalding[17]. The significance of this method can be understood by observing that it is identical with the central-difference scheme for small values of the Peclet-number and otherwise, it reduces to the upwind scheme. For space saving, only the discretized form of the first term of the momentum equation in X-direction by this technique is explained here.

$$\text{First Term} = \frac{\partial}{\partial X}\left(U^2 - \frac{1}{Re}\frac{\partial U}{\partial X}\right) \qquad \text{(A-1)}$$

Based on the finite volume method, integrating the above term over each U-cell in the discretized computational domain (Fig. A-1) gives the following equation:

$$First\ term = \int_c^d \int_a^b \frac{\partial}{\partial X}\left(U^2 - \frac{1}{Re}\frac{\partial U}{\partial X}\right)dXdY = [U_b{}^2 - U_a{}^2 - \frac{1}{Re}(\frac{\partial U}{\partial X})_b + \frac{1}{Re}(\frac{\partial U}{\partial X})_a]\Delta Y \quad \text{(A-2)}$$

$$First\ term = [\frac{\dot{U}_E + \dot{U}_P}{2}\frac{U_E + U_P}{2} - \frac{\dot{U}_W + \dot{U}_P}{2}\frac{U_W + U_P}{2} - \frac{1}{Re}\frac{U_E - U_P}{\Delta X(IP)} + \frac{1}{Re}\frac{U_P - U_W}{\Delta X(IP-2)}]\Delta Y(JP) \quad \text{(A-3)}$$

$$= [CE\frac{U_E + U_P}{2} - CW\frac{U_W + U_P}{2} - DE(U_E - U_P) + DW(U_P - U_W)] \quad \text{(A-4)}$$

$$= U_P(\frac{CE}{2} - \frac{CW}{2} + DE + DW) - U_W(\frac{CW}{2} + DW) - U_E(DE - \frac{CE}{2}) \quad \text{(A-5)}$$

Where

$$CE = \frac{\dot{U}_E + \dot{U}_P}{2}\Delta Y(JP),\ CW = \frac{\dot{U}_W + \dot{U}_P}{2}\Delta Y(JP)$$

$$DE = \frac{1}{Re}\frac{\Delta Y(JP)}{\Delta X(IP)},\ DW = \frac{1}{Re}\frac{\Delta Y(JP)}{\Delta X(IP-2)}$$

It should be mentioned that the asterisks have been dropped in equations (A-1) to (A-5) for convenience. Also, $\dot{U}$ denotes the known value of X-component of fluid velocity at previous iteration level. Based on the hybrid method, the following parameters are obtained as the coefficients for the U-velocity components at the neighborhood grid points (east and west) in the discretized X-momentum equation:

$$AW = \left|\frac{CW}{2}\right| + \frac{CW}{2} \text{ if } \left|\frac{CW}{2}\right| \geq DW$$

$$AW = DW + \frac{CW}{2} \text{ if } DW \geq \left|\frac{CW}{2}\right|$$

$$AE = \left|\frac{CE}{2}\right| - \frac{CE}{2} \text{ if } \left|\frac{CE}{2}\right| \geq DE$$

$$AE = DE - \frac{CE}{2} \text{ if } DE \geq \left|\frac{CE}{2}\right|$$

Then the first term of the integrated momentum equation in x-direction is obtained as follows:

$$\text{First Term} = U_P(AE + AW + CE - CW) - U_W AW - U_E AE \quad \text{(A-6)}$$

The same method can be applied for the second terms in the x-momentum equation to obtain its final form based on the hybrid differencing scheme.

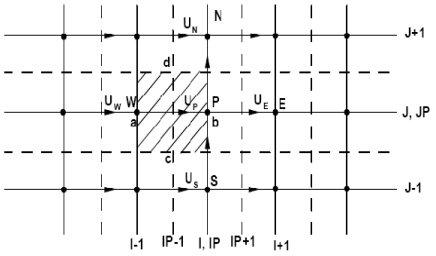

Figure A: 1 U-grid cell

Nomenclature

C_f	friction coefficient
C_f^*	modified friction coefficient
CR	contraction ratio
D_h	hydraulic diameter (m)
ER	expansion ratio

Nu	Nusselt number
Pe	Peclet number
Pr	Prandtl number
Re	Reynolds number
T	temperature (K)
$U_{\circ}$	average velocity of the incoming flow at the inlet section (m/s)
x, y	horizontal and vertical distance, respectively (m)
X, Y	dimensionless horizontal and vertical coordinate, respectively
x_r	reattachment length (m)

Greek symbols

α	thermal diffusivity (m^2/s)
μ	dynamic viscosity ($N.s/m^2$)
ν	kinematic viscosity (m^2/s)
ρ	density (kg/m^3)
Θ	dimensionless temperature
ϕ	step inclination angle

Subscripts

in	inlet section
w	wall
b	bulk value

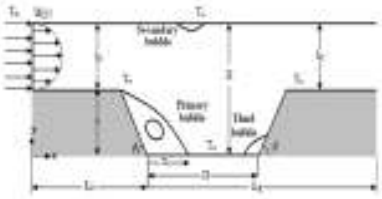

Figure 1: Schematic of computational domain

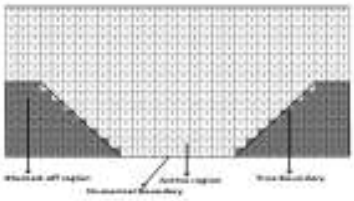

Figure 2: Blocked-off region in a regular grid

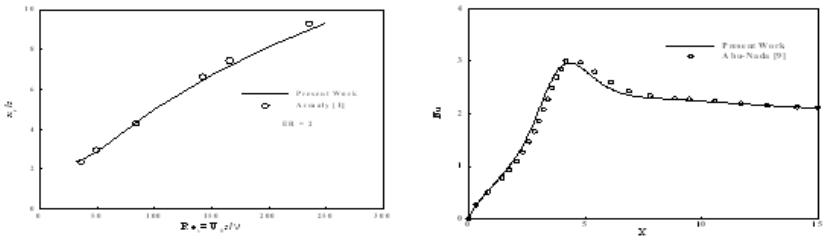

Figure 3: Comparison of numerical results (a) reattachment point, (b) Nusselt number

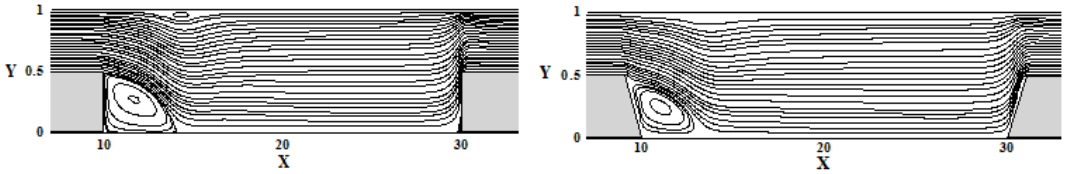

Figure 4: Distribution of stream lines contours, Re = 400, D=20H, (a), (b)

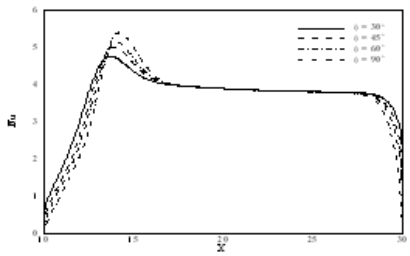

Figure 5: Distribution of Nusselt number along the recess bottom wall, D=20H

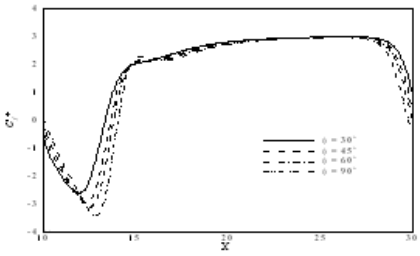

Figure 6: Distribution of modified friction coefficient along the recess bottom wall, D=20H

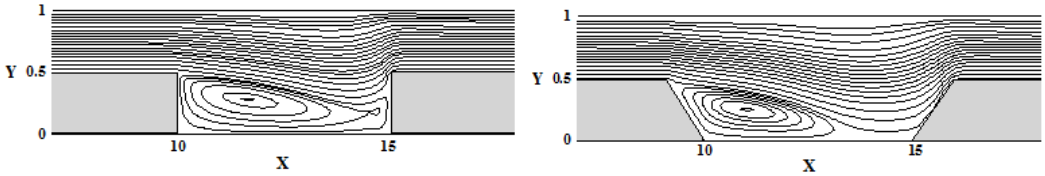

Figure 7: Distribution of stream lines contours, Re = 400, D=5H, (a), (b)

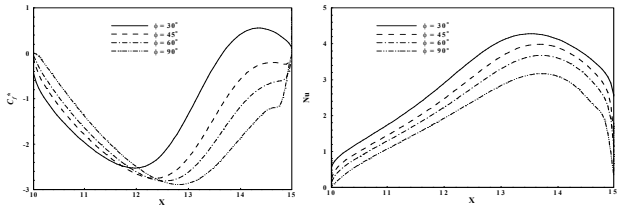

Figure 8: Distribution of modified friction coefficient along the recess bottom wall, D=5H

Figure 9: Distribution of Nusselt number along the recess bottom wall, D=5H

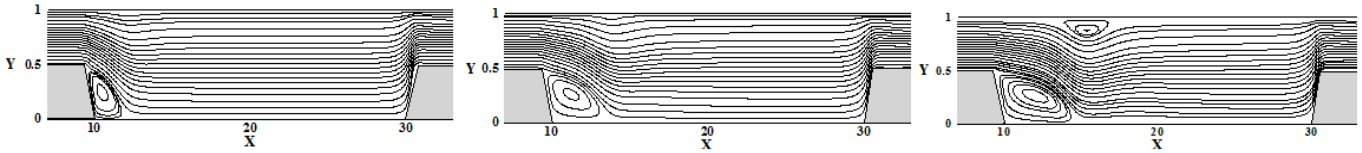

Figure 10: Distribution of stream lines contours,D=20H, (a) Re = 200, (b) Re = 400, (c) Re = 600

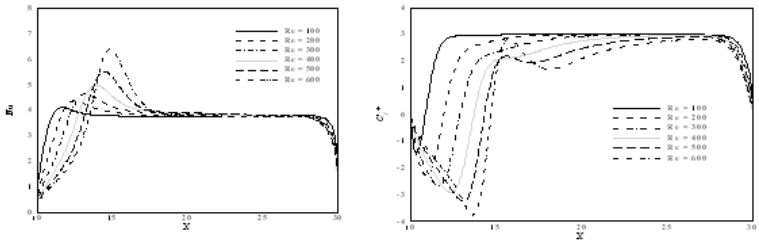

Figure 11: Distribution of Nusselt number along the recess bottom wall, D=20H

Figure 12: Distribution of modified friction coefficient along the recess bottom wall, D=20H

Table 1: Grid independence study, Re=400, D=20H

Grid size	Maximum Nusselt number	x_r / D_h
150×10	0	13.441
350×20	4.556	13.553
550×25	4.733	13.706
700×35	4.885	13.852
800×40	4.990	13.960
850×45	4.992	13.962